Building of a life size testing unit for air conditionning by using TBAB hydrate slurry as a secondary two-phase refrigerant

Jérôme Douzet, Pedro Brantuas, Jean-Michel Herri

BUILDING OF A LIFE SIZE TESTING UNIT FOR AIR CONDITIONNING BY USING TBAB HYDRATE SLURRY AS A SECONDARY TWO-PHASE REFRIGERANT

Jérôme Douzet[1], Pedro Brantuas[1], Jean Michel Herri[1,*]
[1]Centre SPIN, département GENERIC, École Nationale Supérieure des Mines de SAINT-ETIENNE, FRANCE

ABSTRACT

A complete air-conditioning system was built in the "Ecole Nationale Supérieure des Mines" of Saint-Etienne (France). This prototype stands both for a testing unit and for a life-size application. In this installation circulates a crystallized TBAB aqueous solution which presents the ideal physical characteristics for air-conditioning: a melting point adjustable between 0 and 12.3°C and a high latent heat of melting. During the night, the TBAB hydrate slurry is generated and stored in a tank. In the daytime, this slurry is supplied to the air-conditioning heat exchangers. The prototype is instrumented in order to check the energy balances, to study the rheological properties and to monitor the sedimentation in the storage tank. Therefore, a numerical model was proposed to predict the evolution of the hydrates stock in the tank and the available cooling power in function of the tank geometry and the operating conditions. It takes into account hydrate settling, fluid circulation, hydrates formation (in generator) and hydrates melting. Also, we are designing a new type of hydrates generator based on a formation of TBAB-CO_2 semiclathrates that is dissociated in TBAB hydrates in a second step.

Keywords: gas hydrates, quaternary ammoniums, phase change materials

NOMENCLATURE

Cp – Heat capacity ($J.kg^{-1}.K^{-1}$)
C_S – Average solid concentration in the slurry ($kg.m^{-3}$)
$C_{S,0}$ – Solid concentration in the bottom of the column ($kg.m^{-3}$)
D_C – Column Diameter (m)
D_{AB} – Gas diffusion coefficient in the liquid phase ($m.s^{-1}$)
d_0 – Gas injection orifice diameter (m)
$d_{SM,S}$ – Sauter average diameter (m)
g – Standard gravity acceleration constant ($m.s^{-2}$)
h – Height of the hydrate storage tank (m)
k_La – Volumetric mass transfer coefficient (s^{-1})
N – Hydration number (-)
N_0 – Number of orifices for gas injection (-)
P – Power (W)
P_S – Gas vapor pressure (MPa)
P_T – Column pressure (MPa)
Q – Flow rate ($kg.s^{-1}$)
T – Temperature (°C, K)
V_G – Gas superficial speed ($m.s^{-1}$)
Vt – Deposition speed of an hydrate particle ($m.s^{-1}$)
ε_G – Gas holdup (-)
ε_S – Volumetric solid concentration in the slurry (-)
μ_L – Liquid phase viscosity (Pa.s)
μ_G – Gas phase viscosity (Pa.s)
ρ_L – Liquid phase density ($kg.m^{-3}$)
ρ_G – Gas phase viscosity ($kg.m^{-3}$)
ρ_S – Solid phase viscosity ($kg.m^{-3}$)
σ_L – Liquid phase surface tension ($N.m^{-1}$)
υ_L – Liquid cinematic viscosity ($m^2.s$)
φ_S – Volumetric fraction of hydrates in solution (-)

Subscripts:
TBAB – Tetra butyl ammonium bromide

INTRODUCTION

To answer the modern requirements of comfort, the systems of air conditioning are spreading

* Corresponding author: Phone: +33 (0) 4 77 4_2 0_2 9_2 Fax +33 (0) 4 77 49 96 9_2 E-mail: herri@emse.fr

continuously, from the public room to the private houses, passing through the collective buildings. However, such a development has to take into account environmental and economical stakes.

The principle of phase change materials (PCM) is very interesting [1, 2], in terms of environmental stakes: the use of phase change materials allows a reduction of the use of CFC, HCFC and HFC refrigerants, which have a heavy ecological impact. In term of energy, this system harnesses the phenomenon of melting of the solid phase and involves a melting latent heat higher than the sensible heat of a single phase. And finally, the cost of the electrical energy subscription can be smoothed over 24 hours because the slurry is accumulated during the night in an isolated tank.

Phase change materials based on ice slurries have been developed by HeatCraft Europe [3, 4] because of their potential in refrigeration (negative temperature). To that aim, the fluid is composed of water that can crystallize to form ice and the melting point is adjusted by adding appropriate additives, such as alcohols. But, for positive applications, the ice slurry technology is not longer applicable because the melting point cannot be adjusted to positive temperature. In the present work, the PCM is a slurry based on the crystallization of a quaternary ammonium (Tetra-Butyl Ammonium Bromide) that combines to water to form a so-called semi-clathrate, whose melting point can be adjusted up to 12°C. Semi-clathrate is material in which the guest is part of the water lattice. We propose here to experiment this solution at industrial scale in order to test the technology and check the energy balances. Also, we are interested in our capacity to handle the slurry, which means to crystallize it, to store it, and to distribute it. This needs to model the system. In a previous work, Darbouret *et al.* [5] have described and modeled the rheological properties of the slurries. In our work, we focus on the storage tank which is the place of sedimentation. A numerical model is proposed to predict the evolution of the hydrate stock and the available cooling power in function of the tank geometry and the operating conditions. It takes into account hydrate settling, fluid circulation, hydrate formation (in generator) and hydrate melting (in utilization loop and because of heat losses). It can be used to optimize the operating conditions and the geometrical parameters of the hydrate slurry storage tank.

METHODS AND MATERIALS

Principal of the TBAB hydrate slurry air-conditioning system

The thermodynamic properties of an aqueous solution of TBAB are well adapted for an air-conditioning application. Indeed, used as a secondary refrigerant, it can crystallize to form a slurry in which the phase change material is a semi-clathrate compound. With Tetra-n-butyl ammonium bromide, the crystallization temperature can be raised up to 12°C. On the figure 1 we can see the crystallization temperature in function of TBAB mass fraction. The difference between A and B types hydrates consists in the value of hydration number N (respectively 26 and 38). The hydration number is the number of water molecules associated with one molecule of TBAB to form one hydrate.

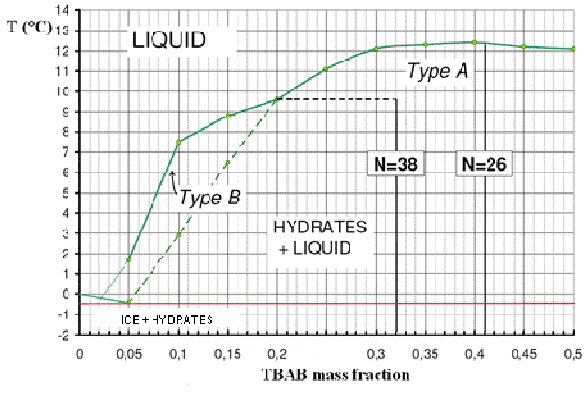

Figure 1: Phase diagram of TBAB hydrates [5].

We built a real size prototype, which stands both for a testing stand and for a life-size application. A compression cycle refrigeration unit (with a condenser installed outside the buildings) allowed via a scraped surface heat exchanger (cooled down by the evaporator) to create TBAB hydrates slurries which were stored in a tank during the night. In the daytime, a pump supplies the slurry to the air conditioning heat exchangers. The capacity of our installation corresponds to the air-conditioning of 4 rooms situated on 3 different floors. Since 2005 the JFE Engineering Corporation (Japan) has shown the feasibility of large-scale utilization of clathrate hydrate slurry for air conditioning [6]. Our research aims to adapt a refrigerating technology for air conditioning in order to give us the know-how and an expertise at

an industrial scale. The principle of our technology consists in using different loops.

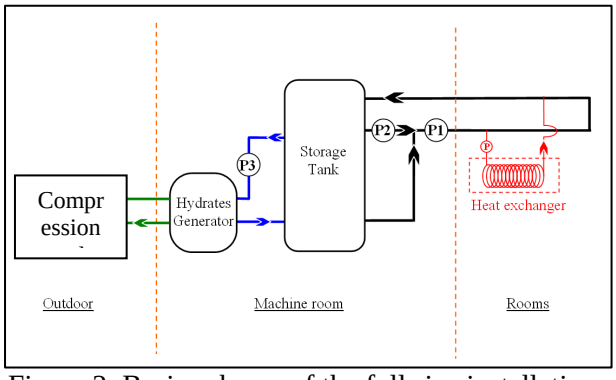

Figure 2: Basic scheme of the full size installation.

The primary loop:

The compression cycle refrigeration unit is connected to the hydrates generator via a refrigerant fluid (R-407C). The hydrates generator crystallizes the aqueous solution of TBAB by recovering the R407C vaporization enthalpy. This compression cycle refrigeration unit is a standard model from LENNOX ®. It is located outside the building. Its cooling capacity is 29,3kW (Electric-power: 13,8kW). It is classically composed of a scroll compressor and a condensing unit, i.e. a heat exchanger that condenses the R407C fluid at ambient temperature. Then the liquefied R407C fluid is directed to the hydrate generator after passing through an expansion valve.

The generating loop:

The aqueous solution of TBAB replaces traditional secondary refrigerant fluids. The hydrates generator transforms the aqueous solution of TBAB into slurry. This hydrates generator is a scraped surface heat exchanger with a capacity of approximately 200L. It was supplied to us by the company HeatCraft (France, 69 Genas) and is usually used to produce ice slurries in the refrigeration field (Ben Lakhdar et al., 2002, 2005).

The slurry is stored in an intermediate tank during the night (when electricity is cheaper). The storage tank communicates with the hydrates generator. The liquid solution is sucked at the top of the storage tank where only liquid is present. In fact, the hydrate particles have a density higher than the liquid, and they settle into the tank. Liquid remains at the top of the tank whereas solids accumulate at the bottom. This tank is approximately 2,5m height and its volume is of about 2m3. It is entirely made of stainless steel.

The distribution loop:

During the day, the slurry is pumped from the storage tank to the secondary loop (by pumps P1 and P2 on the figure 2) and it is melt in heat exchangers located in the room to condition.

The secondary flow loop constitutes the distribution network of the slurry. The slurry is sucked from two different levels of the storage tank. The pump P1(lobes pump) imposes the flow rate. Because it sucks the slurry at the bottom of the storage tank, the solid concentration can be important, up to 40-50% in volume. In order to dilute it, a secondary pump P2 sucks the liquid at the top of the storage tank and injects it just before the pump P1. This allows controlling the volume fraction of solid particles in the slurry of the distribution loop. A volume fraction of 20% was chosen so that viscosity is moderate. The length of this loop is approximately 100m. A flow meter (Coriolis flow-meter from Micro Motion © F) is installed on this loop. The heat exchangers are standard models from LENNOX ®. They are connected on the secondary flow loop with brass pipes, using a little pump installed on each of them. The heat exchangers cool down the air of the room by melting the slurry. 3 floors are conditioned, by the use of 7 heat exchangers (3 on the 1st floor, 2 on the 2nd floor and 2 on the 3rd floor). One of these exchangers is instrumented in order to take measures and to model heat exchanges.

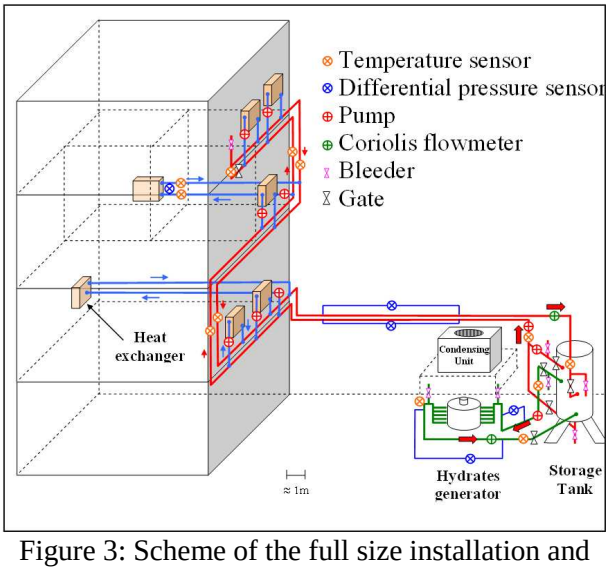

Figure 3: Scheme of the full size installation and location of sensors.

The sensors:
On the figure 3 we can see the localization of some sensors.

Temperature sensors are Pt 100 type. Differential pressure sensors allow measuring the pressure drop during the slurry's circulation this allows to estimate the hydrate fraction in the slurry (Darbouret et al., 2005).
The absolute pressure sensor located near the storage tank is used to verify the slurry height.

System control

For practical reasons, the generation of the hydrate slurry is controlled manually for the moment.
The distribution of the slurry in the rooms is controlled by end-users. In each room, when an end-user activates a heat exchanger, it activates simultaneously the two circulation pumps (P1 and P2).

MODELLING

The experimental study is very time consuming so only a very limited number of configurations (TBAB concentration, operating conditions, geometry of the tank, location of the tank inlets and outlets …) can be investigated. In order to optimize the system a modeling approach was developed to study a large number of configurations by numerical simulation.
One of the crucial phenomena is the settling of the hydrate particles inside the storage tank. Because the hydrate density is higher than that of the solution, hydrate tends to be more concentrated at the bottom of the tank. This can be an advantage because by adjusting the flow rates coming from the bottom and the top of the tank (via the pump P1 and P2), it is possible to adjust the hydrate concentration of the slurry which is supplied to the air-conditioning heat exchangers. Our first experiments were conducted with an eutectic mixture (molar fraction of water corresponding to the hydration number) this is convenient because melting of the hydrate does not change the TBAB concentration in the solution, but melting occurs at the given eutectic temperature of 12.3°C.
However the model was developed to predict variation of TBAB concentration, settling and melting temperature. More generally, it was developed to predict the evolution of the hydrate stock and the available cooling power in function of the tank geometry and the operating conditions (generator and utilization power and flow rate). This needs in fact to predict the evolution of the hydrate slurry state (hydrate fraction, temperature, composition of the residual solution, mean diameter of the hydrate particles) at each height in the tank in function of time.
The main hypotheses are the following: The solution flow and the hydrate settling are vertical. The slurry is homogeneous in a given horizontal section. The volume variation related to hydrate melting is not taken into account and the total height of slurry in the tank is supposed constant (the density difference between the liquid and the solid phase is approximately 40 kg/m3). Nevertheless, the buoyancy forces, depending on density difference, are taken into account in the settling law (Stokes law). The volume of slurry in loops is neglected in comparison with the volume of the tank.
The constitutive equations are concerning the mean velocities of the two phases at a given height, the balance of hydrate particles, the enthalpy balance, the equilibrium curve (figure 1) and the conservation equation of TBAB. The inlets and outlets of the tank correspond to source and sink terms for the conservation equations, which are calculated from the hydrates generation and utilization operating conditions. These constitutive equations were discritised by a semi-implicit finite volume method. Numerical resolution was performed with Matlab ®. The model will be compared with experimental results for validation before its use for system optimization.

PRELIMINARY RESULTS

Handling of the hydrate slurry

Conforming to the results of Darbouret *et al* [5], the distribution of the TBAB hydrate slurry within the secondary loop has not generated difficulties. The volumetric pump (lobes pump) works with the slurry without any difficulty. Concerning the centrifugal pumps, we observed that they work efficiently up to a solid content of 20% vol.

Hydrate generator

The scraped surface heat exchanger was able to produce hydrate slurries with a solid content up to approximately 20 % vol. Figure 4 presents the temperature evolution at inlet and outlet of the

hydrate generator during a typical run where the TBAB solution circulates only in the closed loop between the storage tank and the generator, the solution is at eutectic concentration and the initial temperature is 21°C in the tank.

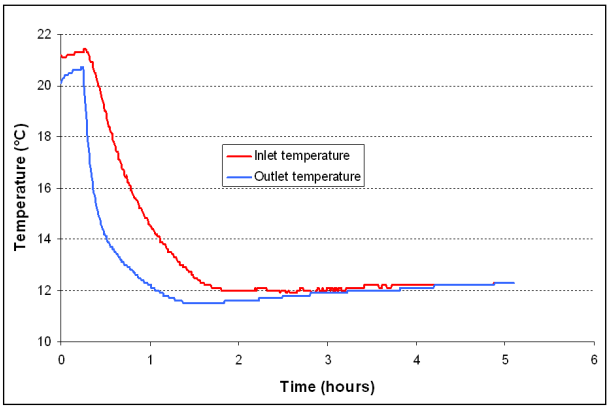

Figure 4: Temperature of slurry at inlet and outlet of the hydrates generator.

During about one hour, the outlet temperature decreases but remains higher than the equilibrium change phase temperature (12.3°C). During this step, the solution remains totally liquid and it is possible to estimate the transmitted power from the temperature and flow rate measurements as follow:

$$P_{TBAB\ solution} = Q_{TBAB\ solution} \cdot Cp_{TBAB\ solution} \cdot (T_{inlet} - T_{outlet}) \quad (1)$$

where $Q_{TBAB\ solution}$ is the TBAB solution's flow rate and $Cp_{TBAB\ solution}$ is heat capacity. The transmitted power decreased from 20 to 7 kW during this first hour.

During a second step, the outlet temperature decreased significantly below 12.3°C, which means that the solution was out of thermodynamic equilibrium. For about 20 min, the temperature decreased (from 12.3°C to 11.5°C) in a similar way as previously and without hydrate generation. Then crystallization began, and the outlet temperature increased progressively up to 12.3 °C.

After about 2 hours, the inlet temperature reached also the phase change temperature. That means that the hydrate generator is fed with a fluid containing already hydrate particles. From this point, the hydrate concentration in the secondary loop (tank, hydrate generator) increases progressively. Consequently, the apparent viscosity and the mechanical friction increases inside the scraped surface heat exchanger. Finally after 5 hours, the rotation of scrapers in the crystallizer is blocked and hydrate generation is stopped. This phenomenon could be explained by the formation of a compact hydrate layer on the heat exchanger plates. It becomes to much thick and difficult to scrape. To prevent the blockage, a solution could be to reduce the temperature difference between the primary refrigerant evaporating temperature (-30°C in our experiment) and the hydrate formation temperature (12,3°C). Another possible solution is to install a system which periodically warms up the hydrate generator in order to eliminate the hydrates accumulated on the plates.

Hydrate storage in the tank

We didn't encounter any problem in the storage of the hydrate slurry. The slurry is maintained in its original state during the storage and it does not agglomerate to form a plug. It is interesting to note that during the winter time and because the ambient temperature decreases at a value lower than 12.3°C, the crystallization can occur spontaneously in the quasi totality of the tank without damaging it. But we observed that pipes can be damaged during melting (molar volume of liquid is superior to solid)

Prediction of the hydrate concentration in the tank

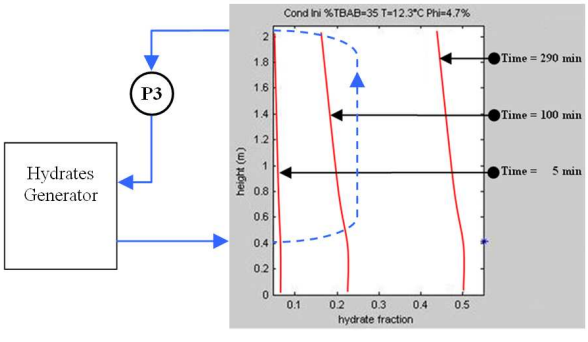

Figure 5: Prediction of hydrate concentration in the tank.

Figure 5 presents an example of the predicted evolution of hydrate volume fraction in function of the height position in the tank for different instants during the generation time (night) for a TBAB concentration of 35%. It can be seen that hydrate concentration increases progressively in the tank. Settling explains that hydrate concentration is

higher at the bottom of the tank and tends to the maximum value of 50% which is a modeling parameter (volume fraction of packed solid particles). The simulation shows that the volume fraction of particles at the top of the tank is in the same order of magnitude than near the bottom. This can be explained by the upward flow in the tank (from h_{inlet}=0.4 m to h_{outlet}= 2m) which compensate the settling phenomena. Indeed, for this concentration of TBAB (35%) the difference of density between the liquid and solid phase is only about 4% so that the settling velocity is low. A practical consequence is that particles are always present at the top of the tank, in concentration which is never negligible. So, the flow which is sucked at the top of the tank and is directed to the crystallizer contains particles, with a volume fraction which increases with time. From an experimental point of view, we have observed this tendency: by sampling the flow before entering the crystallizer we observed an increase of the volume fraction of particles. As a consequence, the viscosity of the slurry increases and the flow rate of the centrifugal pump decreases down to zero. This is an important phenomenon for the design of the pump P3. We have changed it to the profit of a volumetric pump for which the flow rate is less sensitive to the fluid viscosity in the loop.

NEW CO_2 CAPTURE PROCESS

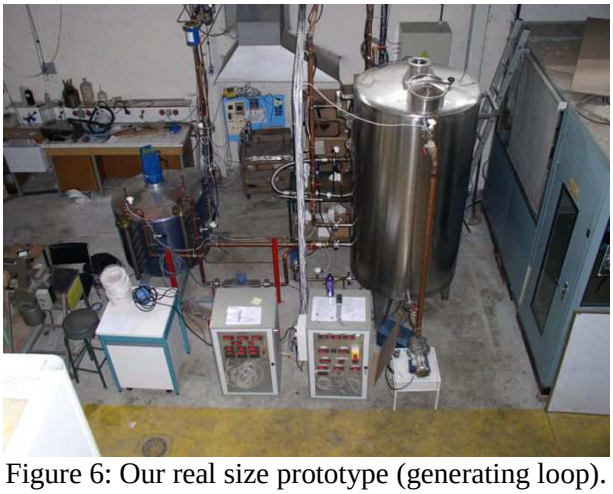

Figure 6: Our real size prototype (generating loop).

We are now in the process of building a new installation for the production of TBAB hydrates. This pilot consists in both capturing CO_2 by hydrate formation and using the formed hydrates for cooling. This is based on the existing setup (Figure 6) where we add a new reactor that is located directly above the hydrates storage.

Figure 7: The CO_2 capture pilot.

The apparatus consists of a bubble column reactor where CO_2 and the TBAB solution comes into contact and forms mixed hydrates of CO_2 + TBAB. The hydrates is then stored until being re-used for the cooling application. The gas is compressed and returned to the bubble column to continue the production of mixed hydrates. This pilot was built with the objective of producing 50 kg/h of mixed hydrates with a gas flow of 2.5 m^3/h and a liquid flow of 1 m^3/h. The reactor works at about 20 bar and 15°C.

Equipments

Figure 7 is the picture of our current pilot located above our other prototype. In left we have our gas compressor/circulator system which consists in 2 ballasts with a volume of about 50 liters and a gear pump in beetween (Figure 8). The CO_2 is provided by 2 bottles situated beneath the gas circulating system. By sucked water from first ballast to the other one, we can push gas to the reactor. We have pressure controllers coupled with automated valves which allows us to have a continuous pumping of gas towards the reactor and extraction from it.

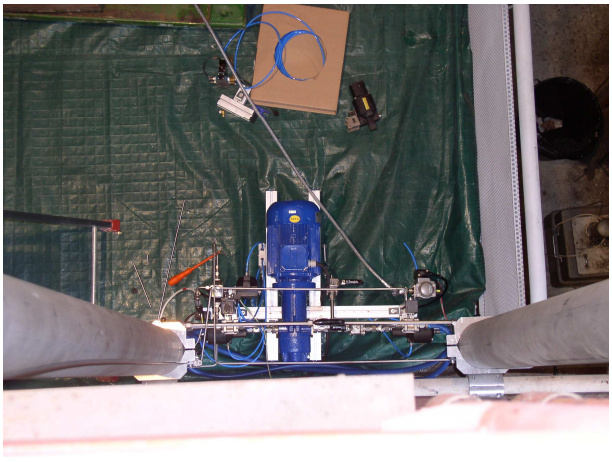

Figure 8: View from the top of the gas circulating device.

In the bottom right we shows our reactor which volume is 50 liters: The reactor has a body made of PMMA to be transparent. It is 2000mm height and diameter of 188mm (Figure 9). The reactor is transparent in order to have a better assessment of gas dispersion phenomena inside the bubble column. After optimization of the gas dispersion system, it will be replaced by a body in 304l steel for having the adequate resistance to the pressure required for the hydrate formation conditions. There is a volumetric pump designed for pumping the hydrates formed between the reactor and the hydrate storage. This pump is placed next to the hydrate storage in a vertical position (Figure 9).

At right of the photo(figure 10) we present the heat exchanger which has 4 meters long and consists of 2 concentric tubes with a counter current flow connected to a cooling device with a power of 3 kW (Figure 10).

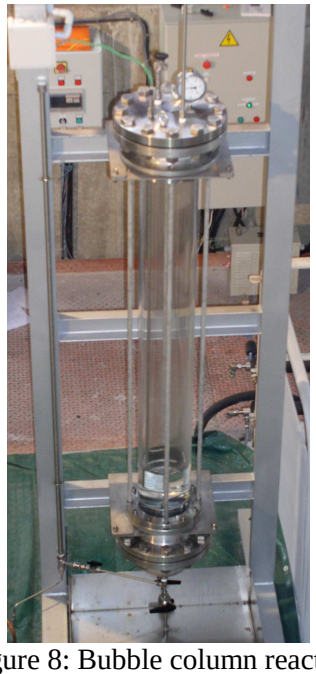

Figure 8: Bubble column reactor.

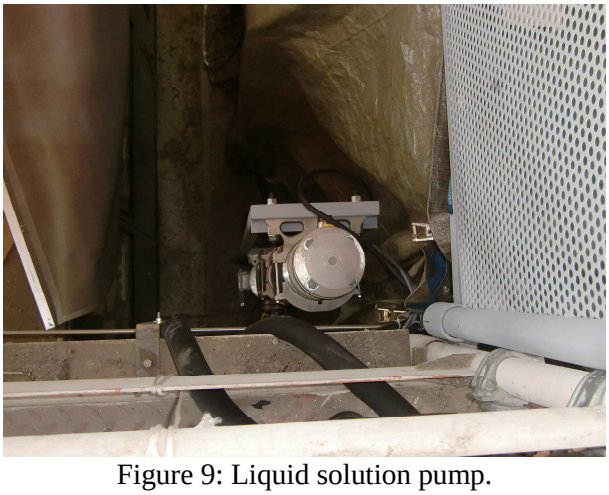

Figure 9: Liquid solution pump.

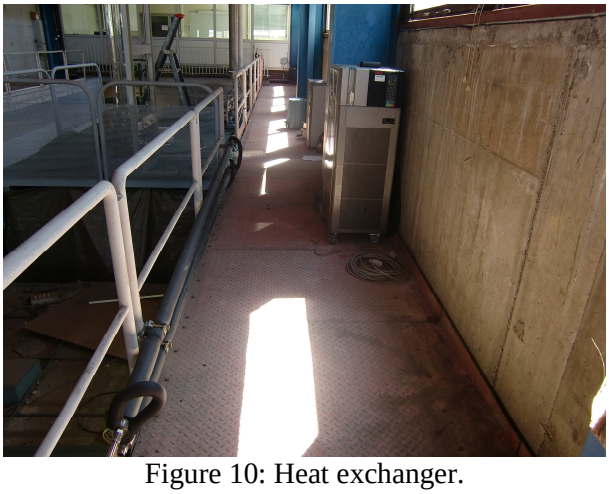

Figure 10: Heat exchanger.

Author	Equations	Reference
Akita & Yoshida	$\frac{\varepsilon_G}{(1-\varepsilon_G)^4} = \alpha\left(\frac{D_C^2\rho_L g}{\sigma}\right)^{1/8}\left(\frac{gD_C^3\rho_L^2}{\mu_L^2}\right)^{1/12}\frac{V_G}{\sqrt{gD_C}}$ $k_L a = 0.6\frac{D_{AB}}{D_C^2}\left(\frac{D_C^2\rho_L g}{\sigma_L}\right)^{0.62}\left(\frac{D_T^3\rho_L^2 g}{\mu_L^2}\right)^{0.31}\left(\frac{\mu_L}{\rho_L D_{AB}}\right)^{0.5}\varepsilon_G^{1.1}$	[7]
Hikita *et al*	$\varepsilon_G = 0.672 f\left(\frac{V_G\mu_L}{\sigma}\right)^{0.578}\left(\frac{\mu_L^4 g}{\rho_L\sigma^2}\right)^{-0.131}\left(\frac{\rho_G}{\rho_L}\right)^{0.062}\left(\frac{\mu_G}{\mu_L}\right)^{0.107}$ $0 < I < 10\ g\cdot ion/l \Rightarrow f = 10^{0.0414I}$ $k_L a = 14.9 g^{0.752} V_G^{0.76}\rho_L^{0.852}\mu_G^{0.243}\mu_L^{-0.079}\sigma_L^{-1.016}D_{AB}^{0.604}$	[8]
Koide *et al*	$\frac{\varepsilon_G}{(1-\varepsilon_G)^4} = \frac{k_1\left(\frac{V_G\mu_L}{\sigma}\right)^{0.918}\left(\frac{g\mu_L^4}{\rho_L\sigma^3}\right)^{-0.252}}{1+4.35(\varphi_S)^{0.748}\left(\frac{\rho_S-\rho_L}{\rho_L}\right)^{0.88}\left(\frac{D_C V_G}{\rho_L}\right)^{-0.168}}$ $k_L a = 2.11\left(\frac{\rho_L D_{AB} g}{\sigma_L}\right)\left(\frac{\mu_L}{\rho_L D_{AB}}\right)^{0.500}\left(\frac{g\mu_L^4}{\rho_L\sigma_L^3}\right)^{-0.159}\varepsilon_G^{1.18}\times$ $\times\frac{1}{1+1.47\times10^4\left(\frac{C_S}{\rho_S}\right)^{0.612}\left(\frac{V_t}{\sqrt{D_C g}}\right)^{0.486}\left(\frac{D_C^2 g\rho_L}{\sigma_L}\right)^{-0.477}\left(\frac{D_C V_G\rho_L}{\mu_L}\right)^{-0.345}}$	[9]
Sauer & Hempel	$\frac{\varepsilon_G}{(1-\varepsilon_G)} = 0.0277\left(\frac{V_G}{(\nu_S g V_G)^{1/4}}\right)^{0.844}\left(\frac{\nu_S}{\nu_{eff,rad}}\right)^{-0.136}\left(\frac{C_S}{C_{S,0}}\right)^{0.0392}$ $\nu_{eff,rad} = 0.011 D_C\sqrt{gD_C}\left(\frac{V_G^3}{g\nu_L}\right)^{1/8}$ $k_L a = C\left(\frac{V_G}{(\nu_{sus} g V_G)^{1/4}}\right)^{n1}\left(\frac{\nu_{sus}}{\nu_{eff,rad}}\right)^{n2}\left(\frac{C_S}{C_{S,0}}\right)^{n3};\nu_{sus} = \frac{\nu_S}{\rho_{sus}}$ $\nu_S = \mu_L\frac{\left(1+2.5\varepsilon_S+10.05\varepsilon_S^2+.00273\exp(16.6\varepsilon_S)\right)}{\rho_S}$	[10]
Chisti	$\frac{k_L}{d_b} = 5.63\times10^{-5}\left(\frac{g\rho_L^2 D_{AB}\sigma_L}{\mu_L^3}\right)^{0.5}\exp(-0.131C_S^2)$ $\frac{k_L}{d_b} = \frac{k_L a_L(1-\varepsilon_G)}{6\varepsilon_G} = \frac{k_L a}{6\varepsilon_G}$	[11]
Behkish *et al*	$\varepsilon_G = 4.94\times10^{-3}\left(\frac{\rho_L^{0.415}\rho_G^{0.177}}{\mu_L^{0.174}\sigma_L^{0.27}}\right)V_G^{0.553}\left(\frac{P_T}{P_T-P_v}\right)^{0.203}\left(\frac{D_C}{D_C+1}\right)^{-0.117}\Gamma^{0.053}\times$ $\times\exp[-2.231\ _S - 0.157(\rho_S d_{SM,S}) - 0.242X_W]$ $\Gamma = (K_d\times N_0 d_0^{\alpha})$ For perforated plates $\zeta = N_0\left(\frac{d_0}{D_C}\right)^2\times100$ X_W = primary liquid mass fraction in the mixture $k_L a = 6.14x10^4\frac{\rho_L^{0.26}\mu_L^{0.12}}{\sigma_L^{0.52}\rho_G^{0.06}}\frac{\varepsilon_G^{1.12}}{V_G^{0.12}d_S^{0.05}}\frac{D_{AB}^{0.50}}{T^{0.68}}\times\Gamma^{0.11}\left(\frac{D_C}{D_C+1}\right)^{0.40}$	[12]

Table 1: List of equations from literature for gas holdup and $k_L a$ for three phase systems in bubble column reactors.

Objectives

Figure 11 shows our gas dispersion tube and also our transparent column with a water solution and air bubbling during our test phase. The presence of three different phases inside the column: liquid (TBAB solution), gas (CO_2) and solid (mixed hydrates) increases the complexity. Especially, bubble columns are equipments which are difficult to design and scale-up due to their complex hydrodynamic behavior. [11, 12, 13 and 14].

Figure 11: Flow of air in a water solution.

A review of the literature concerning three phase system in bubble columns was done in order to find what parameters are determinant in this type of process. Two important parameters are gas holdup (ε_G) and the mass transfer coefficient between the liquid and gas phase (k_La). The gas holdup is the fraction of gas in the liquid phase – the gas bubbles. By analyzing some of the equations from the literature concerning three phase systems in bubble column reactors we have found out that the physical properties of the liquid and solid phase have a strong influence in the gas holdup as well as the gas injection speed into the column. As for the k_La is the gas holdup that shows a bigger influence followed by the gas injection speed and the physical properties of the liquid phase (viscosity, density and surface tension).

CONCLUSIONS

Our experiments demonstrate the feasibility of an air-conditioning system using TBAB hydrate slurry as secondary refrigerant. Some technological problems have still to be solved but different solutions are proposed and will be now tested. A model was developed in order to predict the amount of hydrate and its repartition in the tank. A comparison between numerical and experimental results will be carried out to validate the model. Then the model will be used to simulate new alternatives (other TBAB mass fractions, other inlet and outlet positions, etc.). The best predicted configuration can finally be tested experimentally.

REFERENCES

[1] Oyama H., Shimada W., Ebinuma T., Kamata Y., Takeya S., Uchida T., Nagao J., Narita H.. *Phase diagram, latent heat, and specific heat of TBAB semiclathrate hydrate crystals.* Fluid Phase Equilibria 2005; 234: 131–135

[2] Obata Y., Masuda N., Joo K., Katoh A.. *Advanced technologies towards the new era of energy industries.* NNK technical review 2003; 88: 103-115.

[3] Ben Lakhdar M.A., Melinder A.. *Facing the challenge to produce ice slurry for freezer applications. 5th Ice slurry workshop. May 2002 Stockholm (IIR Paris)*

[4] Ben Lakhdar M.A., Cerecero R., Alvarez G., Guilpart J., Flick, D., Lallemand, A.. *Heat transfer with freezing in a scraped surface heat exchanger.* Applied thermal engineering 2005; 25: 45-60

[5] Darbouret M., Cournil M., Herri, J.M.. *Rheological study of TBAB hydrate slurries as secondary two-phase refrigerants.* International Journal of Refrigeration 2005; 28 (5): 663-671

[6] Mizukami, T., 2010, *Thermal Energy Storage System with Clathrate Hydrate Slurry, JFE Engineering Corporation. Clathrate Hydrates and Technology Innovations, KEIO University « Global COE Program » International Symposium, Yokohama, Japan, March 2010*

[7] Akita, K. and Yoshida, F. *Bubble size, interfacial area and liquid-phase mass transfer coefficient in bubble columns.* Industrial & Engineering Chemistry Process Design and Development 1974; 12: 76-80.

[8] Hikita, H., *et al*. Gas holdup in bubble column. Chemical Engineering Journal And The Biochemical Engineering Journal 1980; 20 (1): 59-67.

[9] Koide, K., Takazawa, A., Kómura, M., & Matsunaga, H. *Gas holdup and volumetric liquid phase mass transfert coefficient in solid suspended bubble columns.* Journal Of Chemical Engineering Of Japan 1984; 17: 459-466.

[10] Sauer, T., Hempel, D.C. *Fluid dynamics and mass transfer in a bubble column with suspended particles*. Chemical Engineering. Technology 1987; 10: 180-189.

[11] Chisti, M.-Y. *Airlift Bioreactors*. New York: Elsevier Science Publishers, 1989.

[12] Behkish, A., Lemoine, R., Oukaci, R., & Morsi, B. I. *Novel correlations for gas holdup in large-scale slurry bubble column reactors operating under elevated pressures and temperatures.* Chemical Engineering Journal 2006; 115: 157 - 171.

[13] Kantarci, N., Borak, F. and Ulgen, K.O. Bubble column reactors. Process Biochemistry, 40, 2005: 2263-2283.

[14] Lemoine, R., Behkish, A., Sehabiaguea, L., Heintza, Y. J., Oukacib, R., & Morsia, B. I. *An algorithm for predicting the hydrodynamic and mass transfer parameters in bubble column and slurry bubble column reactors.* Fuel Processing Technology 2008; 89: 322-343.

ACKNOWLEDGEMENTS

This study benefits of the financial support of the Rhône Alpes region in France.